EUROFUSION WPDIV-CP(16) 15252

JH You et al.

# Progress in the initial design activities for the European DEMO divertor

Preprint of Paper to be submitted for publication in Proceedings of 29th Symposium on Fusion Technology (SOFT 2016)

This work has been carried out within the framework of the EUROfusion Consortium and has received funding from the Euratom research and training programme 2014-2018 under grant agreement No 633053. The views and opinions expressed herein do not necessarily reflect those of the European Commission.

# Progress in the initial design activities for the European DEMO divertor: Subproject 'Cassette'

J.H. You[1]*, G. Mazzone[2], Ch. Bachmann[3], D. Coccorese[4], V. Cocilovo[2], D. De Meis[2], P. A. Di Maio[5], D. Dongiovanni[2], P. Frosi[2], G. Di Gironimo[4], S. Garitta[5], G. Mariano[6], D. Marzullo[4], M.T. Porfiri[2], G. Ramogida[2], E. Vallone[5], R. Villari[2]

[1] Max Planck Institute for Plasma Physics, Boltzmann Str. 2, 85748 Garching, Germany
[2] ENEA Frascati, Department of Fusion and Technology for Nuclear Safety and Security, via E. Fermi 45, 00044 Frascati, Italy
[3] EUROfusion, PMU PPPT Department, Boltzmann Str. 2, 85748 Garching, Germany
[4] CREATE/University of Naples Federico II, Department of Industrial Engineering, Piazzale Tecchio 80 - 80125 Napoli, Italy
[5] Sapienza University of Rome Palazzo Baleani, Dep. of Astronautics, Corso Vittorio Emanuele II, 244 - 00186 Rome, Italy
[6] University of Palermo, Viale delle Scienze, Edificio 6, 90128 Palermo, Italy

Since 2014 preconceptual design activities for European DEMO divertor have been conducted as an integrated, interdisciplinary R&D effort in the framework of EUROfusion Consortium. Being consisted of two subproject areas, 'Cassette' and 'Target', this divertor project (WPDIV) has the objective to deliver a holistic preconceptual design concept together with the key technological solutions to materialize the design. In this contribution, a brief overview on the recent results from the subproject 'Cassette' is presented. In the subproject 'Cassette' the overall system architecture of the Cassette body is engineered based on the baseline CAD model of the European DEMO plant issued in 2015. The preliminary studies being recently completed covered multi-physical analyses including neutronic, thermal, hydraulic, electromagnetic and structural simulations. The most feasible design spaces are identified.

*Corresponding author. Phone: +49 89 3299 1373, Fax: +49 89 3299 1212, Email: you@ipp.mpg.de (Jeong-Ha You)

Keywords: DEMO, Divertor Cassette, EUROfusion, Cooling, Loads, High heat flux

## 1. Introduction.

Since 2014 preconceptual design activities for European DEMO divertor have been conducted in the framework of EUROfusion Consortium. The objective of the divertor project (WPDIV) is to deliver a holistic preconceptual design concept together with the key technological solutions to materialize the design. WPDIV is an integrated, interdisciplinary R&D effort involving six research institutes and 3 universities. WPDIV consists of two subproject areas: 'Cassette design & integration' and 'Target development'. In the subproject 'Cassette' the overall system architecture of the Cassette body is engineered whereas in the subproject 'Target' advanced design concepts and technologies for the plasma-facing target plates are developed [1, 2]. The current design studies are based on the baseline CAD configuration model of the European DEMO plant issued in 2015. The envisaged fusion power is 2037 MW (net electric power: 500 MW). In this contribution, a brief overview on the recent results from the subproject 'Cassette' is presented.

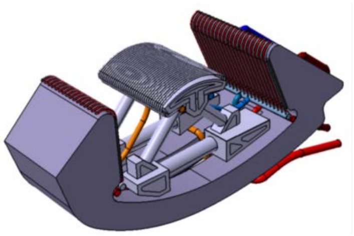

Fig. 1. Schematic design model of the European DEMO divertor Cassette based on the baseline model of the year 2015 [1].

## 2. Neutronic analysis.

For assessment of nuclear heating, irradiation damage and helium transmutation, 3D neutronics calculations were carried out using MCNP5 code and JEFF 3.2 nuclear data. The calculations were normalized to the gross fusion power of 2037 MW which would correspond to a neutron production rate of $7.232 \times 10^{20}$ n/s. It was assumed that the cross section of the plasma-facing component (PFC) consisted of three hypothetical layers where the first and third layers were tungsten while the mid-layer was thought of as a mixture of tungsten (34 vol. %), water (33 vol. %), CuCrZr (18 vol. %) and copper (15 vol. %) representing the actual volume contents of materials in the PFC. For the Cassette body made of Eurofer steel (9Cr1WV), water as well as helium were applied as coolant, for which three different cases of material mixture were considered as follows:

1) $H_2O$-cooled: Eurofer (54 vol. %) + $H_2O$ (vol. 46 %)
2) He-cooled: Eurofer (50 vol. %) + He (50 vol. %)
3) He-cooled: Eurofer (30 vol. %) + He (50 vol. %) + $B_4C$ (20 vol. %)

The $B_4C$ cladding was considered as neutron shielding material. In this preliminary analysis, the dome was not taken into account since the dome design is not consolidated yet. The absence of the dome surely has an impact on neutron wall load and shielding.

### 2.1. Neutron wall loading

In the divertor there is a large spatial variability in neutron wall load. The maximum value amounts to 0.53 MW/m² at the upper surface of the Cassette which corresponds to ca. one half of the maximum neutron wall load at the outboard equatorial first wall (1.33 MW/m$^2$).

### 2.2. Nuclear heating

The nuclear heating power density in the Eurofer steel Cassette ranges from 0.1 to 6 W/cm$^3$ for the water-cooled case whereas it ranges from 0.1 to 4 W/cm$^3$ (3.5 W/cm$^3$ with a $B_4C$ shield) for the helium-cooled case, respectively. The spatial distributions of nuclear heating density are plotted in Fig. 2 for the water-cooled (left) and the helium-cooled (right) cases, respectively. It shows that nuclear heating is concentrated in the middle region of the Cassette and near the PFCs.

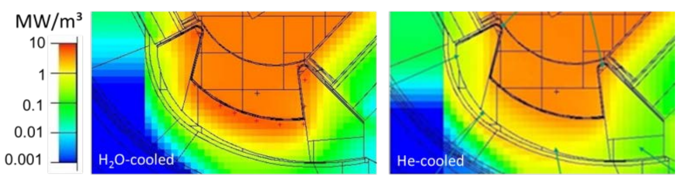


Fig. 2. The spatial distributions of nuclear heating density in the divertor (left: water-cooled, right: helium-cooled).

The total nuclear heating powers in the major components (in 54 Cassettes) are summarized in Table 1. The total nuclear heating power in the entire divertor amounts to 126 MW, 73 MW and 76 MW for the water-cooled, helium-cooled and helium-cooled with a $B_4C$ shield, respectively.

Table 1.

| Nuclear heating in 54 Cassettes (MW) | $H_2O$-cooled ($H_2O$: 46 vol %) | He-cooled (He: 50 vol %) | He + $B_4C$ (20%) (He: 50 vol %) |
|---|---|---|---|
| Inner Vertical Target | 5.4 | 4.9 | 3.8 |
| Outer Vertical Target | 8.1 | 7.0 | 5.4 |
| Dome | 16.7 | 14.0 | 11.3 |
| Cassette Body | 96.1 | 47.0 | 55.6 |
| Total | 126.3 | 72.9 | 76.1 |

2.3. Irradiation damage

The maximum values of dpa (displacement per atom) predicted for the major components of the divertor after 2 fpy (fully power year) and for the vacuum vessel part standing behind the Cassette after 6 fpy are summarized in Table 3. The 2 fpy is the envisaged period of continuous service after which the individual Cassettes will be replaced for maintenance. The data show that the helium-cooled case leads to moderately increased dpa values in the PFCs while the increase of damage due to helium-cooling is substantial in the steel structures (Cassette body, vacuum vessel). In the case of water-cooling, the maximum damage is 3 dpa in the tungsten armor and 13 dpa in the copper heat sink. The maximum damage in the PFCs occurs in the upper region near the blanket and in the dome. The minimum dpa values appear in the lower part of the vertical target where the strike point will likely be located. The peak damage in the Cassette body is 6 dpa. It is thought that the maximum dpa values predicted for the copper alloy and Eurofer steel may be acceptable for structural application in the expected operation temperatures. The fully water-cooled Cassette provides a sufficient neutron shielding for the vacuum vessel (1.8 dpa) while it is not the case in the helium-cooled cases.

Table 2. Irradiation damage predicted for the major components of the divertor after 2 fpy.

| Irradiation damage (dpa/2 fpy) | $H_2O$-cooled ($H_2O$: 46 vol %) | He-cooled (He: 50 vol %) | He + $B_4C$ (20%) (He: 50 vol %) |
|---|---|---|---|
| Eurofer Cassette body | < 6 | < 10 | < 9 |
| Tungsten armor | 1.4 - 3 | < 3.2 | < 3.2 |
| Cu heat sink | 6.4 - 12.8 | < 14.2 | < 14.2 |
| SS 316L vacuum vessel (6 fpy) | < 1.8 | < 4.8 | < 3.9 |

Fig. 3 shows the spatial distributions of irradiation damage rate in the divertor expressed in terms of dpa per fpy (left: water-cooled, right: helium-cooled).

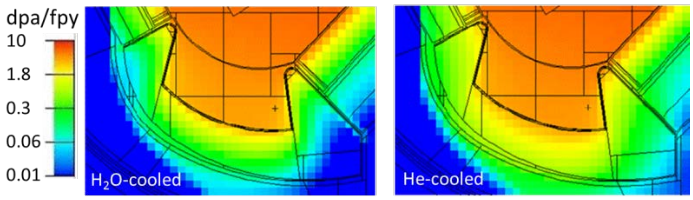


Fig. 3. The spatial distributions of irradiation damage rate (dpa per fpy) in the divertor (left: water-cooled, right: helium-cooled).

2.4. Helium transmutation

Production of helium bubbles as transmutation product has a very critical impact on the structural material since it causes swelling and embrittlement. It also affects the reweldability of the cooling pipes. The helium production rate was assessed for the Cassette assuming austenitic stainless steel (316L) as structural material. The maximum value predicted is 100 appm per 2 fpy. It is noted that the critical limit to allow rewelding of 316L steel is 1 appm. Eurofer will experience a comparable helium production rate as 316L steel owing to the similar boron content. Thus the figure above may be regarded as an approximate estimate for Eurofer Cassette as well. The quite high He production rate indicates that the pipe connections subject to cutting and rewelding operations will have to be located in an outermost outboard region shielded by the blankets and Cassette itself.

2.5. Forthcoming analyses

The next neutronics analysis campaign will include the effect of the dome, real material distribution, different blanket concepts, a more realistic CAD model and the impact of divertor layout on the nuclear heating of the toroidal field magnet coils.

## 3. Cooling scheme and thermohydraulic analysis.

3.1. Operation temperature range for the Cassette body.

It is a fundamental design requirement that the structural material of the Cassette body (i.e. Eurofer) be operated in a ductile state to avoid any uncontrolled fast fracture. In this design study, fracture toughness transition temperature (FTTT) is employed as measure to define the critical temperature band where the material state changes drastically from ductile to brittle. As it is obtained using precracked specimens, FTTT is regarded to be more conservative compared to DBTT (ductile-to-brittle transition temperature) by impact tests. The lower operation temperature limit of irradiated Eurofer can be defined according to the FTTT data at 6 dpa as follows [3]: >180 °C (with He production) or >120 °C (no He production). The upper temperature limit of Eurofer is known to be ca. <550 °C, over which the steel loses strength rapidly. The thermohydraulic design for cooling the Cassette should respect these temperature bounds as compulsory requirements.

3.2. Cassette body cooling.

For the comparative assessment of Cassette cooling performance by two major coolants, water and helium gas, 3D computational fluid dynamics (CFD) analyses were carried out to simulate the thermohydraulic behaviors. Following boundary conditions were assumed as 'starting' parameters.

1) Water-cooled case
Temperature: 150 °C (inlet)
Pressure: 3.5 MPa (inlet)
Mass flow rate: 5.71 kg/s (outlet)

2) Helium-cooled case
Temperature: 350 °C (inlet)
Pressure: 4 MPa (inlet)
Mass flow rate: 1.33 kg/s (outlet)

The interior of the Cassette body is divided into many chambers by rib plates (20 mm thick) each equipped with a hole (diameter: 40-70 mm) through which the pressurized coolant is guided to flow traversing every spaces in the Cassette. A schematic view of the Cassette interior is illustrated in Fig. 4 (a). The outlet and inlet coolant feeding pipes on the outboard edge face are shown. The layouts of the feeding pipes, ribs and holes were optimized on the basis of iterative CFD analyses. The Cassette body has a lattice-like cross section consisting of rectangular chambers in the poloidal direction. The middle poloidal rib separates the inlet and outlet coolant fluxes (see Fig. 4 (b)). The outer shell plate is 30 mm thick.

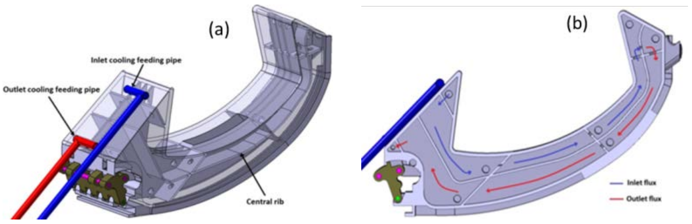

Fig. 4. (a) A schematic view of the Cassette interior with the inlet and outlet coolant feeding pipes on the outboard boundary face, (b) A poloidal cut section of the Cassette where the direction of coolant flow is schematically illustrated.

In Fig. 5, the streamlines of water coolant is plotted together with the speed distribution as color code. In general, the coolant flow exhibits a reasonable streamline pattern, but two large vortices are formed in the outboard region where a further optimization is needed.

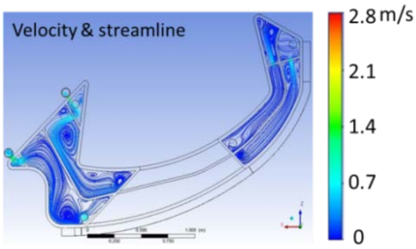

Fig. 5. Streamlines of the water coolant flowing in the divertor Cassette. The speed distribution is indicated by a color code.

The results of the CFD analysis are summarized in Table 3 both for the water-cooling and helium-cooling cases. It is found that the water-cooling case exhibits a superior thermal and hydraulic performance compared to the helium-cooling case. Particularly, water-cooling is definitely beneficial in terms of pumping power costs compared to helium-cooling by more than a thousand times (4 kW vs. 5 MW). The temperature range building in the water-cooled Cassette seems nearly optimal for Eurofer steel while the temperature range in the helium-cooled Cassette largely exceed the desired upper temperature limit of Eurofer (550 °C). In the water-cooled Cassette, the coolant bulk is heated up to 220 °C in the outlet region. The maximum temperature in the water coolant reaches locally up to 242 °C in the thin boundary layer forming at the solid wall which is close to the vaporization temperature at the given pressure. Water mass flow rate needs to be increased to lower the maximum coolant temperature increasing the margin to film boiling.

Table 3. Predicted thermal and hydraulic performance of water-cooled and helium-cooled divertor Cassette.

| | $H_2O$-cooled | He + $B_4C$ (20%) |
|---|---|---|
| Pressure drop [MPa] | 0.01 | 0.21 |
| Pumping power (total) | 4.1 kW | 5.0 MW |
| Coolant max. temp. [°C] | 242 (wall)/220 (bulk) | 610 |
| Cassette body temp. [°C] | <350 (max. 415) | <750 (max. 810) |

3.3. Target plate cooling.

The thermohydraulic performance of water-cooled divertor target plate was assessed by means of 3D CFD simulations. The target plates are PFCs exposed to high heat flux loads generated by radiation (53 MW), plasma bombardment (39 MW) and nuclear heating (30 MW). This means that 54 in- and outboard target plates have to exhaust the deposited thermal power of 122 MW in total. At the strike point the maximum power density can reach about 20 MW/m² during slow transients (plasma reattachment) in a few seconds. During a quasi-stationary operation the maximum power density is expected to reach 10-15 MW/m² [2]. The power exhaust capability has to be assured in terms of the global energy balance as well as local margin to critical heat flux (CHF) at the wall. To fulfill the requirement, a highly efficient cooling scheme and technologies for materializing reliable PFCs are demanded.
To this end, three different options of cooling scheme have been devised and estimated (Fig. 6). The boundary conditions assumed as starting parameters are as follows:

- Surface heat flux: 17 MW/m²
- Heat flux peaking factor: 2
- Coolant temperature: 150 °C (inlet)
- Coolant pressure: 5 MPa (inlet)
- Mass flow rate per pipe: 1.67 kg/s

Fig. 6. Three different cooling scheme options considered for the thermohydraulic design of the divertor target plate.

The results of the comparative CFD analysis are summarized in Table 4. All three options seem to allow sufficient margin to the CHF at the strike point for the applied load. It is noted that the recommended margin to CHF is 1.4 at least. The rise of coolant temperature looks also moderate for all three cases. On the other hand, the pressure drop is quite significant. Another concern is the very high coolant speed which may foster pipe wall erosion. The outcome of this CFD analysis implies that the mass flow rate needs to be substantially reduced while decreasing the inlet water temperature at the same time in order to reduce the pressure drop and speed without compromising the margin to CHF. Currently, a follow-up investigation is ongoing targeting the coolant speed of about 10 m/s, pressure drop below 1.4 MPa and CHF margin higher than 1.4. Here, the recommended operation temperature range for the irradiated CuCrZr alloy cooling tube (13 dpa) will set the bound for the inlet coolant temperature. Such temperature range needs to be confirmed by the dedicated structural design rules.

Table 4. Thermohydraulic performance of water-cooled divertor target plate predicted for three different cooling options.

| per Cassette | Option 1 | Option 2 | Option 3 |
|---|---|---|---|
| Total mass flow rate (kg/s) | 60 | 110 | 60 |
| Temperature rise (°C) | 9 | 5 | 9 |
| Pressure drop (MPa) | 1.4 | 1.5 | 1.8 |
| min. Velocity (m/s) | 17 | 15 | 15 |
| min. CHF margin | 1.6 | 1.6 | 1.4 |

## 4. Electromagnetic force analysis.

Macroscopic plasma instabilities such as plasma disruptions and vertical displacement events (VDE) induce considerable transient electric currents in the conductive steel body of the divertor. The disruptions generate eddy currents in the toroidal direction while the VDEs produce halo currents in the poloidal direction. These currents interact with the magnetic field generating mechanical forces in vertical direction (Lorentz force: $\vec{F}=\vec{J}\times\vec{B}$). Particularly, the force induced by a VDE may impose a significant impact on the divertor due to strong current density. In order to assess this type of impact loads, extensive electromagnetic analyses were carried out making empirical assumptions on the halo fraction, toroidal peaking factor and the repartition coefficient to correlate the amplitude of halo currents to the strength of plasma current. Contact resistance between the parts was neglected. The nominal toroidal magnetic field was assumed to be 5.7 T. The minimum and maximum toroidal magnetic field during a VDE is estimated to be 5.6 and 8.3 T, respectively.

### 4.1. Halo currents

The electric potential builds up along the poloidal path from the inboard to the outboard side. The maximum magnitude reaches up to ca. 825 V/m. The halo current density in the Cassette body bulk ranges mostly from -3 to 3 MA/m² both in the vertical and radial directions. Concentration of current density occurs at the shell edges and corners.

### 4.2. Lorentz forces and stresses

The induced Lorentz forces in the shell plate are plotted in Fig. 7 (left: vertical, right: radial component). Strong upward vertical force appears in the middle part of the Cassette body (30 MN) and downward vertical force in the inboard and outboard wings (10 MN). The upward vertical force causes (elastic) deformation of the middle part where the displacement reaches up to 1.4 mm upwards.

Fig. 8 shows the induced stress fields (von Mises stress) in the outer shell plate (left) and in the internal ribs (right). The stress state in the entire Cassette structure remains in the elastic regime even in the most severe loading case considered in this analysis. This result indicates that the Cassette body is robust enough to withstand the transient electro-mechanical impact loads caused by envisaged plasma VDEs.

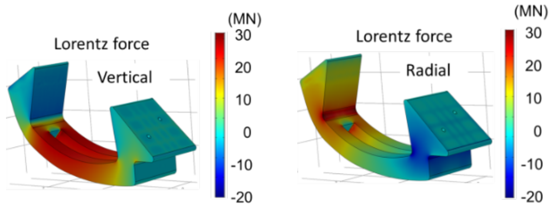


Fig. 7. Induced Lorentz forces in the divertor Cassette shell plate (left: vertical, right: radial component).

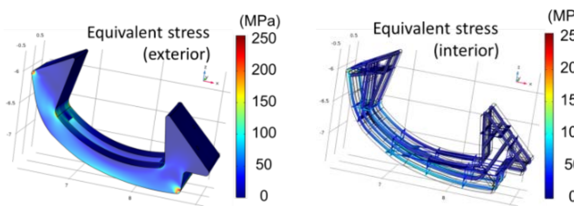


Fig 8 shows the induced stress field (von Mises equivalent stress) in the shell plate (left) and in the internal ribs (right).

## 5. Structural analysis.

The stress intensities produced by electromagnetic impact loads during a VDE (type 3) were evaluated and used for assessing the structural failure criteria as formulated in the French code RCC-MRx. The results are summarized in table 5. It may be deferred that the severe VDE would not lead to serious structural failure.

Table 5. Structural failure criteria estimated for impact loads due to a VDE (type 3) based on RCC-MRx code.

| | | | |
|---|---|---|---|
| Monotonic loading by a single VDE (RCC-MRx) | | | |
| $P_m+P_b$ (path 1) | 47 (MPa) | $S_m$ | 280 (MPa) |
| $P_m+P_b$ (path 2) | 60 | $1.5{\cdot}S_m$ | 280 |
| Cyclic loading by repeated VDEs (RCC-MRx) | | | |
| $Max(P_m+P_b)+\Delta Q$ (Path 1) | 158 | $3{\cdot}S_m$ | 560 |
| $Max(P_m+P_b)+\Delta Q$ (Path 2) | 128 | $3{\cdot}S_m$ | 560 |

## 6. Supports and fixation scheme.

Five different design concepts have been considered to develop a Cassette fixation scheme and to design the static supports. Two of them (with preloading) are illustrated in Fig. 9. Each concept is associated with benefits and disadvantages. Possible inelastic deformation of the fixation keys due to irradiation swelling, halo current heating or impact loads is one of the critical concerns. A further study is ongoing focusing on kinematics and fabrication.

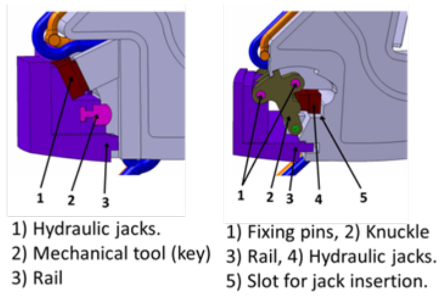


Fig. 9. Two selected examples of Cassette fixation scheme using static supports (with preloading).

## 7. Summary.

Recently, the European DEMO divertor project has successfully completed the preliminary design space exploration phase and is entering into a consolidation phase. In the subproject 'Cassette', the preconceptual design studies worked through specification of physical and structural loads for different coolant media, thermal and hydraulic optimization of cooling schemes and invention of fixation schemes.

## Acknowledgment

"This work has been carried out within the framework of the EUROfusion Consortium and has received funding from the Euratom research and training program 2014-2018 under grant agreement No 633053. The views and opinions expressed herein do not necessarily reflect those of the European Commission."

## References

[1] J.H. You, G. Mazzone, E. Visca et al., Fus. Eng. Des. 109-111 (2016) 1598-1603.
[2] J.H. You, E. Visca, Ch. Bachmann et al., Nucl. Mater. Ener. (2016) doi: 10.1016/j.nme.2016.02.005.
[3] E. Gaganidze J. Aktaa, Fus. Eng. Des. 88 (2013) 118-128.